Elastic light scattering from nucleated blood cells: rapid numerical analysis

P. M. A. Sloot and C. G. Figdor

A model is presented to calculate the light-scatter properties of nucleated blood cells which are mimicked by two concentric spheres. The light-scatter characteristics were derived from the Rayleigh-Debye-Gans approximation and by simultaneous application of field averaging of the internal field and modification of the propagation constant inside the different cellular compartments. It is shown that the results obtained with this simple model are similar to those obtained with more complex and more exact theories. In addition it is demonstrated that simultaneous detection of the light-scatter intensities in the forward-, lateral-, and backscatter directions is required to optimize the detection of different cell types in heterogeneous populations of nucleated blood cells.

I. Introduction

Light scattered from nucleated blood cells contains information on both the cell size and of the morphology of the cell.[1–4] This nondestructive sensing of a single cell has led to numerous analytical and preparative applications in cell biology.[1,5–10] The number of theories describing light scatter from biological cells is, however, limited. Rayleigh scattering cannot be applied to mammalian cells, since this theory holds only for particles with a size comparable to the wavelength of the incident light, whereas the size of nucleated blood cells is much larger (3–40-μm diameter). Various other theories have been developed to describe elastic light scattering beyond the Rayleigh domain.[11,12] Most models proposed so far, such as the fundamental Mie theory[13] and derivatives thereof,[14] are based on the Maxwell equations and regard light scattering as a boundary value problem. However, these models have a number of serious disadvantages. The computational schemes resulting from the Mie theory are complicated and time-consuming,[15] although improvement of the speed of calculation is sometimes possible.[16,17] The theories are difficult to interpret and provide information which is far beyond experimental accuracy.[18,19] In addition, the Mie theory describes elastic light scattering based on a homogeneous spherical body of arbitrary size and refractive index, whereas nucleated blood cells are inhomogeneous (cytoplasm, nucleus) and may be irregularly shaped. Therefore coated sphere models[20–22] are much more realistic since they can account for intracellular heterogeneities. However, these models result in even more complex algorithms.[20,23,24] In this study we propose a spherical shell model which describes elastic light scattering from a single particle with the dimensions of a nucleated blood cell in a modified Rayleigh-Debye-Gans approximation. The results demonstrate that this simplified theory closely resembles the more complex theories and that it is well suited to approximate the elastic light scattering of nucleated blood cells of various shapes and sizes, especially in flow cytometry. In contrast to other studies where large vector-processing computers (IBM CDC 6600 or 7600) are required for calculations,[16,24] all the data presented in this study could be calculated by means of a microcomputer (HP 9845; BASIC interpreter).

II. Theory

The model proposed here is based on the Rayleigh-Debye-Gans approximation (or Born approximation), where the scatterer is considered as a particle constructed by Rayleigh scattering volumes and the phase shift is added for each volume dV. Only single scattering and elastic scattering are studied. The angular intensity of the scattered radiation is given by

$$I(\Theta) = I_0 \frac{i_1(\Theta) + i_2(\Theta)}{2k_0^2 R^2}, \quad (1)$$

where $i_n(\theta) = |S_n(\theta)|$ and Θ = angle of detection. The

The authors are with Netherlands Cancer Institute (Antoni van Leeuwenhoek Huis), Biophysics Division, Plesmanlaan 121, 1066 CX Amsterdam, The Netherlands.

Received 27 March 1986.
0003-6935/86/193559-07$02.00/0.

scatter functions $S_n(\theta)$ result from perpendicular ($n = 1$) or parallel ($n = 2$) polarized incident light relative to the plane of scattering. I_0 represents the intensity of the incident light. The distance from the particle to the point of observation is givenby R, and k_0 is the propagation constant of the applied field outside the particle and is defined by $k_0 = (2\pi/\lambda_0)$, where λ_0 is the wavelength of the incident light in vacuum. The form factor $P(\Theta)$ contains all the information on cellular size, shape, and refractive index $[m(r)]$ and is defined by

$$\left.\begin{matrix} S_1(\Theta) \\ S_2(\Theta) \end{matrix}\right\} = ik_0^3\alpha(r)P(\theta)\begin{cases}1\\ \cos(\Theta)\end{cases} \tag{2}$$

The polarizability $\alpha(r)$ describes the changes in the charge distribution of the particle induced by the oscillating electromagnetic field. Interference from the waves emerging from the total volume V is described by $P(\Theta)$:

$$P(\Theta) = \frac{1}{v}\int_v |m^2(r) - 1| \exp\left[ik_0 r 2 \sin\left(\frac{\Theta}{2}\right)\right] dv, \tag{3}$$

from which it is clear that $P(\Theta)$ can be considered as the Fourier transform of the refractive-index function: $|m^2(r) - 1|$ with $m(r)$ relative to the surrounding medium. The internal field can be replaced by the incident field if the relative refractive index is ~1 and the phase shift is sufficiently small.[11,12] Shimizu[25] showed that modification of the propagation constant of the electromagnetic field in the particle, for waves to (applied field) and from (induced scattered field) the scattering volume dV, can be accomplished by insertion of the relative refractive index into the Fourier kernel of Eq. (3). In this case the limitations on phase shift and on relative refractive index are less stringent, which makes it possible to define light scatter of a large entity such as a nucleated blood cell. Therefore in Eq. (3) k_0 is replaced by $k_0 \cdot m(r)$.

A collection of concentric spheres can now be described by

$$P(\Theta) = \frac{1}{\alpha(r)}\int_0 4\pi r^2 a'(r) \frac{\sin\left[2k_0 m(r) r \sin\left(\frac{\Theta}{2}\right)\right]}{2k_0 m(r) r \sin\left(\frac{\Theta}{2}\right)} \cdot dr, \tag{4a}$$

where the volume polarizability $\alpha'(r)$ is defined by

$$\alpha(r) = \int_v \alpha'(r) dV. \tag{4b}$$

The volume polarizability inside the structured sphere may be approximated by the volume weighted average of the polarizability of a homogeneous sphere[22]:

$$\frac{\bar{m}^2 - 1}{\bar{m}^2 + 2} = \frac{1}{V}\int_V \frac{m^2(r) - 1}{m^2(r) + 2} dV = M_0. \tag{5}$$

A nucleated blood cell can be mimicked by two concentric spheres where the nucleus represents the inner sphere (radius a; relative refractive index m_a) and the cytoplasm represents the outer sphere (radius b; relative refractive index m_b) (Fig. 1).

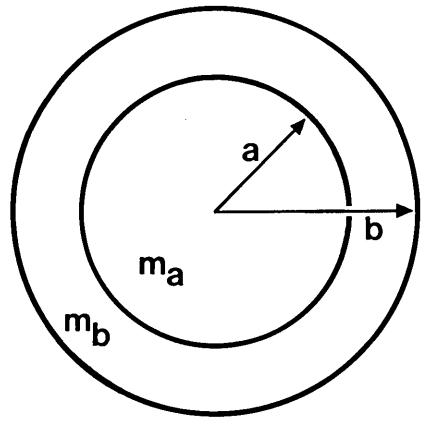

Fig. 1. Concentric sphere model for nucleated cells: m_a and m_b are the relative refractive indices, a and b are the radii of the inner and outer spheres, respectively.

Integration of Eq. (5) with respect to r regarding the boundary values of the relative refractive indices,

$$m(r) = \begin{cases} m_a & 0 < r \le a, \\ m_b & a < r \le b, \end{cases}$$

results in

$$M_0 = \frac{1}{V_b}[M_a V_a + M_b(V_b - V_a)], \tag{6}$$

where $M_a = (m_a^2 - 1)/(m_a^2 + 2)$ and the volume of the nucleus $V_a = (4/3)\pi a^3$. M_b and V_b are defined similarly. The mean polarizability for the inhomogeneous sphere is given by $\bar{\alpha} = b^3 M_0$ and the polarizability of the nucleus equals $\alpha_a = a^3 M_a$. Therefore the volume polarizability of the cytoplasm and the nucleus can be derived by integration of Eq. (4b), which results in

$$\alpha_a' = \frac{3}{4} M_a \text{ and } \alpha_b' = \frac{b^3 M_0 - a^3 M_a}{V_b - V_a}. \tag{7}$$

Subsequently the form factor $P(\Theta)$ is calculated by integration of Eq. (4a):

$$P(\Theta) = \frac{(2\pi)^{3/2}}{\alpha(r)}\left\{\alpha_a' \frac{a^3}{U_1^{3/2}} J_{3/2}(U_1) + \alpha_b' \frac{b^3}{U_2^{3/2}} J_{3/2}(U_2) - \frac{a^3}{U_3^{3/2}} J_{3/2}(U_3)\right\}, \tag{8}$$

where $U_1 = 2ak_o m_a \sin(\Theta/2)$,
$U_2 = 2bk_o m_b \sin(\Theta/2)$,
$U_3 = 2ak_o m_b \sin(\Theta/2)$.

Since scatter functions are normally described in terms of Bessel functions,

$$\frac{1}{U^3}[\sin(u) - u\cos(u)] \text{ is replaced by } \left[\frac{\pi}{2U^3}\right]^{1/2} J_{3/2}(U)$$

in Eq. (8), where $J_{3/2}(U)$ represents the three half order Bessel functions.[26] The heterogeneity implied in Eq. (8) can be removed by adjusting the radius a and/or refractive index m_a. In the limit $a \to 0$ or $m_a \to m_b$ or $a \to b$, Eq. (8) result in

$$\underset{\text{homogeneous}}{P(\theta)} = \left[\frac{2\pi}{U_2^3}\right]^{1/2} J_{3/2}(U_2).$$

This equation is equal to the modified Rayleigh-Debye-Gans approximation for a homogeneous sphere.[25]

III. Elastic Light Scattering from Spherical Cells of Various Size, Optical Density, and Nucleus/Cytoplasm Ratio

We applied the derived form factor $P(\Theta)$ [Eq. (8)] to investigate the influence of the various scatter function parameters on the differential scatter intensities of human peripheral blood leukocytes (e.g., lymphocytes). These calculations provide information on the relationship between forward light scatter (FS), side scatter (SS), and backscatter (BS). Most experimental systems measure FS and SS.[5–7] FS is considered to be proportional to cell size, whereas SS has been shown to provide information on the internal structure of the cells.[4,9] In addition BS is studied because it is only in this region that reflection is the predominant scatter mechanism. Since light scatter is always measured at finite scatter angles, determined by the sensitive area of the detector (e.g., photomultiplier tube) and the distance between the detector and the scattering entity, we present our calculations in terms of integrated signals which are typical for most experimental systems.[2,7,19]

The numerical calculations were carried out by means of the trapezoidal rule[26]:

$$\text{forward scatter (FS) } I_{FS} = \int_{1°}^{7°} I(\Theta)d\Theta,$$

$$\text{side scatter (SS) } I_{SS} = \int_{76°}^{104°} I(\Theta)d\Theta,$$

$$\text{backscatter (BS) } I_{BS} = \int_{160°}^{180°} I(\Theta)d\Theta.$$

Furthermore, both the distance to the detector and the intensity of the incident radiation are unity.

The light-scatter intensities were integrated with respect to the scatter angle Θ, which is defined parallel to the scatter plane. Differential effects for scatter angles perpendicular to the scatter plane were discarded since large spheres near the diffraction limit exhibit complete rotational symmetric light-scatter intensities. Nevertheless, some weak differential effects have been reported by Sharpless *et al.*[27]

Since we are especially interested in light scattering from nucleated blood cells (e.g., lymphocytes), the size and refractive indices of the nucleus and the cytoplasm are restricted.[21,24,28] The size of the radius of the outer sphere is $1\ \mu m \leq b \leq 7\ \mu m$; the relative refractive indices are $1 + 10^{-6} \leq m_a, m_b \leq 1 + 10^{-1}$, and $m_a > m_b$.

The ratio of the radius of the inner sphere/outer sphere is 3.0/3.5 μm since this represents a typical value for human peripheral blood lymphocytes. Finally, we assumed that the incident light was provided by a He–Ne laser (λ = 632.8 nm) and the cells were irradiated in an aqueous solution (refractive index = 1.333). Furthermore, to be able to compare our results with those obtained in other studies,[20,21,22] the incident light was assumed to be polarized parallel with respect to the scatter plane.

In this paper no absorption effects were studied for the following reasons:

(i) The wavelength of light emerging from a He–Ne laser is 632.8 nm, therefore no significant absorption is expected when blood cells are irradiated.[29]

(ii) The results of this theory were compared with two other approximation models,[22,24] where absorption has also been discarded.

(iii) For a weakly absorbing sphere, the absorption cross section is proportional to its volume.[18] Since we are especially interested in morphological differences in terms of differences in $m(r)$ throughout one and the same volume, no additional relevant information is expected. Therefore we applied real-valued relative refractive indices in our calculations.

Four different situations were examined (Figs. 2–5) which covers all the information that can be extracted from this model, if small changes in size and morphology are studied in relation to FS, SS, and BS. First, the influence of the ratio a/b on the light-scatter spectrum is calculated. Second, we calculated the increase of the total cell size (b) at a constant ratio a/b. Finally, changes in the optical density of the cytoplasm and the nucleus are studied independently.

Figure 2 shows the effect of different nucleus/cytoplasm size ratios on the light scattered in the three principal directions (FS, SS, BS). The data demonstrate that both the number of extrema and the differences in top-to-top intensities of the irradiance are much larger for BS in comparison with SS, which indicates that the BS signal reveals much more information than the SS signal. In addition it is shown that the magnitude of the overall intensity in the BS direction is ten times higher than in the SS direction. Finally, it can be read from Fig. 2 that the information provided by FS is negligible.

Calculations at other refractive indices indicate the same tendency for FS, SS, and BS (data not shown). For large particles (e.g., blood cells) the impact of changes in nucleus/cytoplasm ratio on the scattered light can be explained in terms of geometrical optics.[21] FS is expected to be mainly determined by diffraction at the cytoplasm membrane and nucleus membrane. Since the refractive indices of nucleus and cytoplasm are close to one another it can be assumed that changes in the cytoplasm/nucleus size ratio cannot be detected in a forward scatter direction. SS, however, is determined by both refraction and diffraction and therefore the ratio a/b becomes important in the lateral regions. BS is assumed to consist of mainly (multiple) reflection and refraction, which implies that minor changes in the size ratio result in large changes in the BS intensities.

Next we considered a situation in which the nucleus/cytoplasm ratio a/b was kept constant whereas the total cell size increased. The results shown in Fig. 3 demonstrate that FS and SS vary within the same range of intensities. A linear plot of the FS intensity vs the increment of the nucleus/cytoplasm size ratio can be fitted to a polynomial of the fourth degree. Statistical analysis (chi-square test) showed a good fit

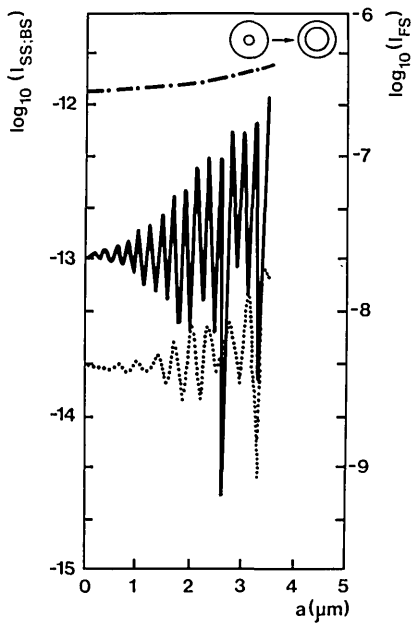

Fig. 2. Logarithm (base 10) of the integrated intensity function $I(\theta)$ for FS, · – · – · – ·; SS, ...; BS, —— vs the size of the inner sphere. The outer sphere is held constant at 3.5-μm radius; $m_a = 1.10$; $m_b = 1.08$.

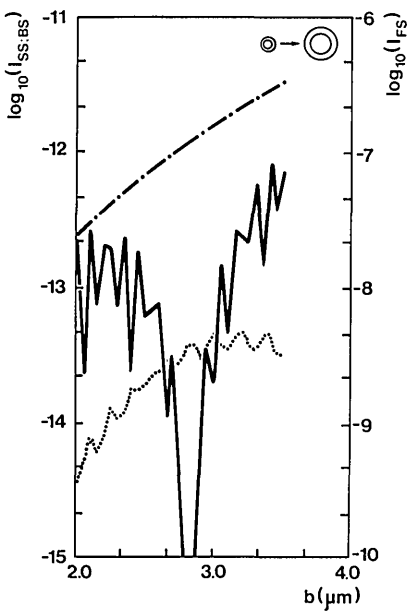

Fig. 3. Logarithm (base 10) of the integrated intensity function $I(\theta)$ for FS, · – · – · – ·; SS, ...; BS, —— vs the size of the sphere. The ratio a/b is 3.0/3.5; $m_a = 1.10$; $m_b = 1.08$.

(~98%). It was found that both optical density and changes in nucleus/cytoplasm ratios have only minor effects on the polynomial. From this it can be concluded that FS may be used to predict gross cell size as has already been suggested by many authors. However, it has to be kept in mind that the degree of the polynomial is also determined by the optics of the scatter device, the shape of the beam of incident light, and the beam stop as was shown by Steinkamp *et al.*[30]

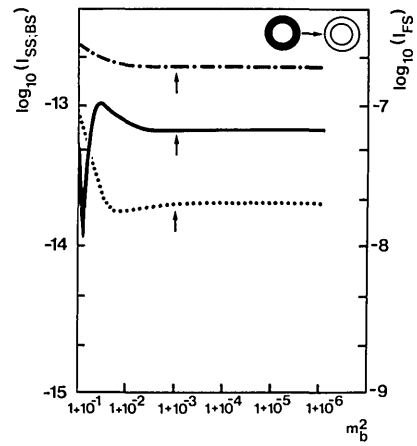

Fig. 4. Logarithm (base 10) of the integrated intensity function $I(\theta)$ for FS, · – · – · – ·; SS, ...; BS, —— vs the decrease of the square of relative refractive index of the cytoplasm (m_b^2). The ratio a/b is 3.0/3.5, and $m_a^2 = 1.21$. The arrows indicate the value of m_b^2 below which no information of changes in optical density is available.

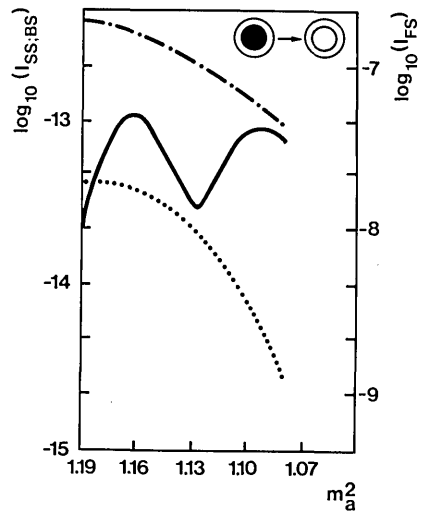

Fig. 5. Logarithm (base 10) of the integrated intensity function $I(\theta)$ for FS, · – · – · – ·; SS, ...; BS, —— vs the decrease of the square of the relative refractive index of the nucleus. The ratio a/b = 3.0/3.5 and $m_b^2 = 1.05$.

SS, similar to FS, also increased in intensity in parallel with cell size (Fig. 3). However, in contrast to FS a number of extrema are superimposed on this monotone rising intensity function. Similarly large fluctuations are also observed in the backscatter direction. The light-scatter intensities measured at various nucleus/cytoplasm ratios showed a very large minimum at a cell size of 2.85 μm. Further calculations (not shown) demonstrated that there is not distinct relation between the site of the minimum and the various cellular parameters. This phenomenon is likely to be the result of destructive interference.

Finally, changes in the differential scatter intensities induced by small changes in the optical density of the cytoplasm and the nucleus were studied in two independent situations. In the first place the influence of decreasing optical density of the cytoplasm at a

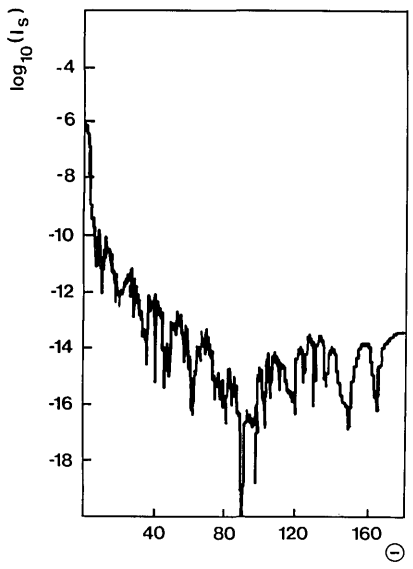

Fig. 6. Logarithm (base 10) of the relative scatter intensity function $I(\theta)$ vs θ for a coated sphere with $\alpha = (2/3)\beta$, $\beta = 85$, $m_a = 1.05$, and $m_b = 1.03$. The incident light is polarized parallel to the scatter plane.

fixed transparency of the nucleus on the scatter intensities was calculated (Fig. 4). The graph shows that FS is insensitive to any changes in the optical density of the cytoplasm. This is a consequence of the small differences in refractive index between the surrounding medium and the cytoplasm. Therefore FS in this situation is mainly determined by the cellular size. Furthermore, the data indicate that SS and BS are approximately equally sensitive to changes in m_b. The parameters FS, SS, and BS reach a constant intensity at $m_b \cong 1 + 10^{-3}$ which is independent of further decrease in optical density. This suggests that beyond this value of m_b scatter measurements reveal no information of relative changes in optical density. Calculations carried out at other values of m_a and/or nuclear size resulted in the same detection limit (data not shown). Second, we studied the effect of a decrease in optical density of the nucleus at a fixed transparency of the cytoplasm on the scattered light. The calculations showed that in this situation FS is sensitive to small changes in m_a. SS, however, is approximately twenty times more sensitive than is FS (Fig. 5). The oscillating function for BS has a typical maximum at $m_a^2 \cong 1.16$. The site of this first maximum is independent of m_b or the ratio a/b (data not shown). This implies that BS is exclusively related to changes in optical density of the nucleus.

IV. Comparison with Other Scatter Models

In this section we examine the similarity of the model with two other more complex approximations.[22,24] To be able to compare the various theories, the incident light was assumed to be polarized parallel with respect to the scatter plane. Furthermore the size parameters a and b are expressed as α and β defined by $(2\pi a)\lambda$ and $(2\pi b)\lambda$, respectively. In Fig. 6 the differential scatter intensities vs the complete range of scatter angles Θ are shown. Note that the intensity drops dramatically at $\Theta = 90°$. This is a fundamental consequence of the model applied, since the $\cos(\Theta)$ term in Eq. (2) equals zero. Since the number of envelopes and the angular sites of the high frequency components contain all the information,[21] only (dis)similarities of these quantities with the results obtained by Brunsting and Mullaney[24] are shown in Table I.

In addition we compared the proposed model with the formal Aden-Kerker solution (AK) in the small concentric sphere limit where the latter is valid.[20,22] In the first place we considered the lateral and backward directions. It can be read from Fig. 7 and Table

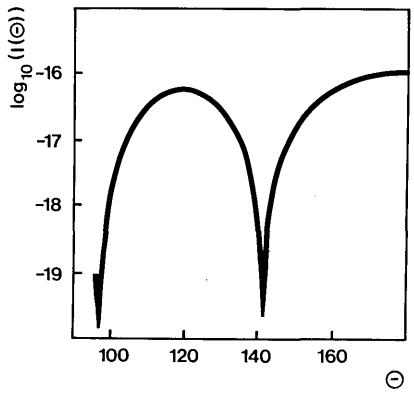

Fig. 7. Logarithm (base 10) of the relative scatter intensities $I(\theta)$ vs θ ($\theta \geq 95°$) for $\alpha = 1.75$, $\beta = 7$, $m_a = 1.10$, and $m_b = 1.0583$.

Table I. Comparison of the Scatter Spectrum Between the Proposed Model and the Literature: Brunsting *et al.*[24] for Particles with $\alpha = (2/3)\beta$, $\beta = 85$, $m_a = 1.05$, and $m_b = 1.03$ (see also Fig. 6)

	Number of envelopes		Intensity range		$[\Delta \log_{10}(I_s)]$ from $\Theta = 0°$ to 90°		from $\Theta = 90°$ to 180°		
Proposed model	10		Proposed model		0; −16		−16		
Literature	10		Literature		0; −8		−8		
Low frequency minima (degrees)									
Proposed model	20	31	48	60	69	90	119	117	
Literature	16	28	43	56	72	79	108	140	
Typical minima (degees)									
Proposed model	3	11	41	79	90	98	—	149	165
Literature	4	—	—	79	—	103	108	150	161

Table II. Comparison of the Scatter Spectrum ($\Theta \geq 95°$) Between the Proposed Model and the Exact Small Spherical Shell Model: Kerker[22] $\alpha = 1.75$, $\beta = 7$, $m_a^2 = 1.21$, and $m_b^2 = 1.12$ (see also Fig. 7)

Extrema	Proposed model				AK solution			
Number	1	2	3	4	1	2	3	4
Type	Min	Max	Min	Max	Min	Max	Min	Max
Site (degrees)	97	119	141	180	110	120	141	180
Magnitude [$\log_{10}(I_s)$]	−19.8	−16.3	−19.6	−16.0	−16.8	−16.4	−19.0	−15.9

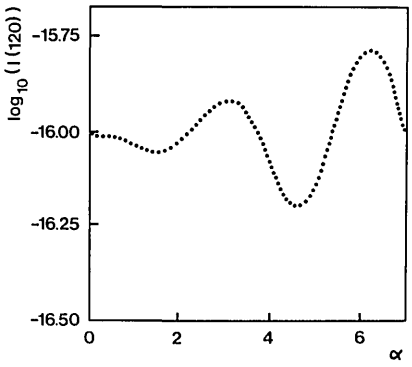

Fig. 8. Logarithm (base 10) of the relative scatter intensity at $\theta = 120°$ for $\beta = 7$, $0 \leq \alpha \leq 7$, $m_a = 1.10$, and $m_b = 1.0817$.

produce a complete spectrum ($\Theta = 0°$ to 180°; $\Delta\Theta = 0.5$) is ~30 s when the programs are written in BASIC. It is obvious that the computational time may be reduced to a fraction of this mean time when real-time languages, e.g., ADA or ASSEMBLY, in a processor configuration with a high clock frequency, are applied.[31] Furthermore, calculation time of Mie-like algorithms increase dramatically with increasing size parameter, whereas the computational time for the proposed model is independent of the particle size.

(ii) The model can be applied to large entities such as nucleated blood cells (2–20-μm diameter).

(iii) The integral representation of the form factor $P(\theta)$ completely describes the scatter phenomena in this model. Replacement of k_0 by $k_0 \cdot m(\bar{r})$ and $m(r)$ by $m(\bar{r})$ (the relative refractive index represented by a vector) in Eq. (3) and modification of Eq. (5) for nonspherical structures,[12] permits calculations of less symmetrical cell morphologies. Accordingly more realistic geometrical representations of the cell shape can be calculated (such as the enucleated biconcave discocyte shape of an erythrocyte or cells such as polymorphonuclear leukocytes).

Table III. Comparison of the Scatter Intensities ($\Theta = 120°$) Between the Proposed Model and the Exact Small Spherical Shell Model: Kerker[22] $\beta = 7$, $0 \leq \alpha \leq 7$, $m_a^2 = 1.21$, and $m_b^2 = 1.17$ (see also Fig. 8)

Extrema	Proposed model				AK solution			
Number	1	2	3	4	1	2	3	4
Type	Min	Max	Min	Max	Min	Max	Min	Max
α	1.6	3.1	4.7	6.2	1.6	3.2	5.0	6.7
Magnitude [$\log_{10} I(120°)$]	−16.1	−15.9	−16.2	−15.8	−16.2	−16.0	−16.7	−16.2

II that the intensity range of the proposed model is equal to the exact AK values. The minimum at 97°, however, is much more pronounced and is expected to be at 110°. The site and magnitude of the minimum at 141° equals the AK solution. Calculation of the variations of the scatter intensities at $\Theta = 120°$ with respect to small changes in the scatter parameter α (Fig. 8, Table III) showed a close resemblance to the formal solutions.

V. Conclusions

In this study we proposed a model to describe the scattering of a plane monochromatic wave by a nucleated blood cell. We showed that given the modification of the field inside the particle and volume weighted averaging of the polarizability, the Rayleigh-Debye-Gans approximation may be applied to calculate the light-scatter spectrum if small variations in cellular parameters are considered. The model is consistent with more complex and more restricted theories and has a number of additional advantages:

(i) The simple computational scheme [Eqs. (1) and (8)] allows high speed calculation of the differential scatter intensities, which is of great importance for the on-line interpretation of light-scatter measurements carried out in flow (5000 cells/s). The mean time to

The proposed model has been used to study small well-defined changes in the cellular parameters on experimentally determined forward-, side-, and backscatter signals. It can be derived from these calculations that FS is mainly determined by gross cell size regardless of the nucleus/cytoplasm ratio. However, it was observed that changes in the refractive index of the nucleus also affected FS. In contrast, SS is sensitive to all the changes studied in the morphology of the cell. BS is determined by the nucleus/cytoplasm ratio and changes in the optical density of the cytoplasm and of the nucleus. The results strongly suggest a direct correlation between the transparency of the nucleus and the intensity of the BS signal. All three principal directions were found to be insensitive to changes in the optical density of the cytoplasm at relative refractive-index values smaller than $1 + 10^{-3}$.

To be able to detect small differences in the morphology of nucleated blood cells with a heterogeneity

in optical density, it is required that the observed scatter angles must contain additional and mutually independent information. Most light-scatter instruments (e.g., flow cytometers) used for the differentiation of biological cells measure forward scatter vs fluorescence or forward scatter vs side scatter. The results presented here indicate that simultaneous detection of FS, SS, and BS should be applied to obtain optimal optical resolution if heterogeneous populations of nucleated blood cells are studied.

Further studies will be required to determine the influence of variations in shape, different detection angles, and ratio of detection angles on the light-scatter spectrum. This information together with the data presented has been used to develop a three-parameter light-scatter device for real-time detection of human peripheral blood leukocytes in flow (manuscript in preparation). The relative simple computational algorithm which results from the proposed model facilitates tuning of the various parameters of the model to the measured light-scatter intensities.

We thank J. v. d. Elsken (University of Amsterdam) and W. S. Bont for critical reading of the manuscript D. Besselsen for fruitful discussions, and Marie Anne van Halem for secretarial help. This work was supported by Stichting Technische Wetenschappen (STW), grant LGN-22053.

References

1. A. W. S. Richie, R. N. Gray, and H. S. Mickle, "Right Angle Light Scatter: a Necessary Parameter in Flow Cytofluorimetric Analysis of Human Peripheral Blood Mononuclear Cells," J. Immunol. Methods **64,** 109 (1983).
2. J. W. M. Visser, G. J. van der Engh, and D. W. Van Bekkum, "Light Scattering Properties of Murine Hemopoietic Cells," Blood Cells **6,** 391 (1980).
3. M. Kerker, "Elastic and Inelastic Light-Scattering in Flow Cytometry," Cytometry **4,** 1 (1983).
4. M. C. Benson, D. C. McDougal, and D. S. Coffey, "The Application of Perpendicular and Forward Light Scatter to Assess Nuclear and Cellular Morphology," Cytometry **5,** 515 (1984).
5. G. C. Salzman *et al.*, "Cell Classification by Laser Light Scattering: Identification and Separation of Unstained Leukocytes," Acta Cytol. **19,** 374 (1975).
6. M. K. Loken and A. M. Stall, "Flow Cytometry as an Analytical and Preparative Tool in Immunology," J. Immunol. Methods **50,** 85 (1982).
7. J. A. Steinkamp, "Flow Cytometry," Rev. Sci. Instrum. **55,** 1375 (1984).
8. G. C. Salzman *et al.*, "A Flow-System Multiangle Light-Scattering Instrument for Cell Characterization," Clin. Chem. N.Y. **21,** 1297 (1975).
9. Y. C. Smart, J. Cox, B. Murphy, A. Enno, and R. C. Burton, "Flow Cytometric Enumeration of Absolute Lymphocyte Number in Peripheral Blood Using Two Parameters of Light Scatter," Cytometry **6,** 172 (1985).
10. J. Yuli and R. Snyderman, "Rapid Changes in Light Scattering from Human Polymorphonuclear Leukocytes Exposed to Chemoattractants," J. Clin. Invest. **5,** 1408 (1984).
11. M. Kerker, *The Scattering of Light and Other Electromagnetic Radiation* (Academic, New York, 1969).
12. H. C. van de Hulst, *Light Scattering by Small Particles* (Dover, New York, 1981).
13. G. Mie, Ann. Phys. **25,** 377 (1908).
14. S. Asano and G. Yamamoto, "Light Scattering by a Spheroidal Particle," Appl. Opt. **14,** 29 (1975).
15. J. V. Dave, "Subroutines for Computing the Parameters of the Electromagnetic Radiation Scattered by a Sphere," Report 320.3237 (IBM Scientific Center, Palo Alto, CA, 1968).
16. W. J. Wiscombe, "Improved Mie Scattering Algorithms," Appl. Opt. **19,** 1505 (1980).
17. A. R. Jones, "Calculation of the Ratios of Complex Rircatti-Bessel Functions for Mie Scattering," J. Phys. D. **16,** L49 (1983).
18. C. F. Bohren and T. J. Nevitt, "Absorption by a Sphere: a Simple Approximation," Appl. Opt. **22,** 774 (1983).
19. M. R. Melamed, P. F. Mullaney, and M. L. Mendelsohn, Eds., *Flow Cytometry and Sorting* (Wiley, New York, 1979).
20. A. Aden and M. Kerker, "Scattering of Electromagnetic Waves from Two Concentric Spheres," J. Appl. Phys. **22,** 1242 (1951).
21. R. A. Meyer and A. Brunsting, "Light Scattering from Nucleated Biological Cells," Biophys. J. **15,** 191 (1975).
22. M. Kerker, D. D. Cooke, H. Chew, and P. J. McNulty, "Light Scattering by Structured Spheres," J. Opt. Soc. Am. **68,** 592 (1978).
23. P. W. Barber and C. Yeh, "Scattering of Electromagnetic Waves by Arbitrarily Shaped Dielectric Bodies," Appl. Opt. **14,** 2864 (1975).
24. A. Brunsting and P. F. Mullaney, "Light Scattering from Coated Spheres: Model for Biological Cells," Appl. Opt. **11,** 675 (1972).
25. K. Shimizu, "Modification of the Rayleigh-Debye Approximation," J. Opt. Soc. Am. **73,** 504 (1983).
26. M. Abramowitz and I. A. Stegun, Eds., *Handbook of Mathematical Functions* (Dover, New York, 1970).
27. T. K. Sharpless, M. Bartholdi, and R. Melamed, "Size and Refractive Index Dependence of Simple Forward Angle Scattering Measured in a Flow System Using Sharply-Focused Illumination," J. Histochem. Cytochem. **25,** 845 (1977).
28. H. Begemann and J. Rastetter, *Atlas of Clinical Hematology* (Springer-Verlag, New York, 1979).
29. P. Latimer, D. M. Moore, and F. D. Bryant, "Changes in Total Light Scattering and Absorption Caused by Changes in Particle Conformation," J. Theor. Biol. **21,** 348 (1968).
30. J. A. Steinkamp, M. J. Fulwyer, J. R. Coulter, R. D. Hiebert, J. L. Horney, and P. F. Mullaney, "A New Multiparameter Separator for Microscopic Particles and Biological Cells," Rev. Sci. Instrum. **44,** 1301 (1973).
31. J. V. Cugini, "Selection and Use of General-Purpose Progamming Languages, Computer Science and Technology," Natl. Bur. Stand. (U.S.) Spec. Publ. 500-117 (1984).